Shine-Through in PET/MR Imaging: Effects of the Magnetic Field on Positron Range and Subsequent Image Artifacts

Armin Kolb[1], Alexander W. Sauter[2], Lars Eriksson[3], Arne Vandenbrouke[4], Chih C. Liu[1], Craig Levin[4], Bernd J. Pichler[1], and Magdalena Rafecas[1]

[1]Werner Siemens Imaging Center, Department of Preclinical Imaging and Radiopharmacy, Eberhard Karls University, Tübingen, Germany; [2]Department of Radiology, Eberhard Karls University, Tübingen, Germany; [3]Siemens Medical Solutions, Knoxville, Tennessee; and [4]Molecular Imaging Program at Stanford University, Stanford, California

Simultaneous PET/MR imaging is an emerging hybrid modality for clinical and preclinical imaging. The static magnetic field of the MR imaging device affects the trajectory of the positrons emitted by the PET radioisotopes. This effect translates into an improvement of the spatial resolution in transaxial images. However, because of the elongation of the positron range distribution along the magnetic field, the axial resolution worsens and shine-through artifacts may appear. These artifacts can lead to misinterpretation and overstaging. The aim of this work was to study the relevance of this effect. **Methods:** Measurements were performed in a 3-tesla PET/MR scanner. A 1-cm^2 piece of paper, soaked with a radioisotope and placed in air, was scanned, and the magnitude of the shine-through was quantified from the PET images for various radioisotopes. Additionally, PET/MR and PET/CT images of the lungs and the larynx with trachea of a deceased swine were obtained after injecting a mixture of $NiSO_4$ and ^{68}Ga to simulate hot tumor lesions. **Results:** For the radioactive paper, shine-through artifacts appeared in the location of the acrylic glass backplane, located 3 cm from the source in the axial direction. The ratio between the activity of the shine-through and the activity reconstructed in the original location ranged from 0.9 (^{18}F) to 5.7 (^{68}Ga). For the larynx-with-trachea images, the magnitude of the artifacts depended on the organ orientation with respect to the magnetic field. The shine-through activity could reach 46% of the reconstructed activity (larynx lesion). The lesion within the trachea produced 2 artifacts, symmetrically aligned with the magnetic field and characterized by artifact-to-lesion volume-of-interest ratios ranging from 21% to 30%. **Conclusion:** In simultaneous PET/MR imaging, the effect of the magnetic field on positrons may cause severe artifacts in the PET image when the lesions are close to air cavities and high-energy radioisotopes are used. For accurate staging and interpretation, this effect needs to be recognized and adequate compensation techniques should be developed.

Key Words: PET/MRI; artifact; positron-range; high-energy positrons; shine-through

J Nucl Med 2015; 56:951–954
DOI: 10.2967/jnumed.114.147637

PET/MR imaging is a powerful technology that is now expanding worldwide (*1*); integrated PET/MR imaging systems are already commercially available for clinical applications (*2,3*). Special attention is thus being paid to the ability of simultaneous PET/MR imaging to provide quantitative information and artifact-free images. A particular phenomenon of this integrated technology is the effect of the static magnetic field on positrons. Because of the Lorentz force, positrons follow helical paths along the magnetic field lines. Consequently, the positron range distribution narrows in the plane perpendicular to the magnetic field, thus improving the transaxial resolution (*4–9*). On the other hand, little attention has been devoted to the behavior of positrons in the axial direction. The positron range distribution elongates along the magnetic field, and the axial resolution subsequently degrades (*9–11*). The positron range can reach up to a few millimeters in air, and "positron beams" may be created (*12*). Depending on the lesion location, the strength of the magnetic field, the positron energy, and the density of the surrounding tissues, severe artifacts may distort the image. In addition to axially elongated activity distributions, there may be a shine-through artifact (*13–15*)—an apparent activity concentration visible in the reconstructed image on the other side of an air cavity, diametrically opposed to the location of the true lesion. Abduhl-Fatah et al. (*13*) showed that these artifacts were observed in PET/CT because of the large positron range of ^{124}I. In PET/MR imaging, this phenomenon may become more relevant because of the Lorentz force, and the artifacts may also appear for less energetic radioisotopes. It is thus fundamental to identify those scenarios in which positron shine-through may occur, endangering accurate quantification and diagnosis. With this goal in mind, we tested various radioisotopes in different scenarios, including animal tissues, and quantified the apparent activity.

MATERIALS AND METHODS

PET/MR Imaging Scanner

The measurements were performed with a clinical brain PET/MR imaging system (BrainPET, Tim Trio MR; Siemens Healthcare). The PET scanner (*16*) was mounted inside a 3-tesla MR scanner. The spatial resolution in the center was 2.3, 3.1, and 2.6 mm in full width at half maximum in the *x, y,* and *z* directions, respectively (*16*). Acquired list-mode data were reconstructed using an ordinary Poisson ordered-subsets expectation maximization 3-dimensional algorithm (6 iterations and 16 subsets) (*17*). The *z*-axis of the scanner was defined as aligned with the magnetic field. Additional measurements were performed with a clinical PET/CT (*18*) Hi-Rez Biograph 16 (Siemens Medical Solutions) with a spatial resolution of about 4 mm.

Received Aug. 27, 2014; revision accepted Jan. 19, 2015.
For correspondence contact: Armin Kolb, Werner Siemens Imaging Center, Department of Preclinical Imaging and Radiopharmacy, Eberhard Karls University, Tübingen, Röntgenweg 13, 72076 Tübingen, Germany.
E-mail: armin.kolb@med.uni-tuebingen.de
Published online Mar. 12, 2015.

TABLE 1
Main Characteristics of Isotopes and Activities Calculated from Phantom Measurements

Isotope	Half-life (min)	Maximum e^+ energy (keV)	Paper (%)	Backplane (%)	B/P
^{18}F	109.7	635	52.4	47.6	0.9
^{11}C	20.3	960	43.7	56.3	1.3
^{13}N	9.97	1,190	31.1	68.9	2.2
^{68}Ga	68.3	1,895	14.9	85.1	5.7

B/P = backplane-to-paper ratio.

Phantom Measurements

A thin 1-cm^2 piece of paper (80 g/m^2) was soaked with common PET isotopes (Table 1) and fixed with a surgical fiber into an acrylic glass device (Fig. 1). The device was centered at the field of view, and the paper was placed parallel to the backplane of the device (orthogonal to the magnetic field); the distance between the paper and the backplane was 30 mm. From the reconstructed 3-dimensional images, the percentages of annihilation events that originated on the paper and on the backplane were estimated and a backplane-to-paper ratio was calculated. For this purpose, profiles were extracted from the corresponding coronal planes, and the relative area below the profiles was calculated.

Measurements of Swine Organs

The lungs and the larynx with trachea from a deceased swine were separately fixed onto Styrofoam (The Dow Chemical Co.). A liquid solution consisting of 1 mL of glue, 1 mL of $NiSO_4$, and 0.1 mL of ^{68}Ga was produced. The glue was used to create a high-viscosity medium, whereas the $NiSO_4$ provided a hyperintense MR signal in T1-weighted sequences. The lungs were inflated with oxygen and sealed at the trachea. Three types of lesions were created. To simulate hot pulmonary lesions, the radioactive solution was injected with a syringe in 5 different locations inside the lungs (0.1 mL/lesion); the same volume was applied by submucosal injection into the lower medial part of the epiglottis. Finally, to simulate a tumor with infiltration into the trachea, a thin balloon combined with a catheter was filled with 0.2 mL of the aforementioned solution and placed through a cut within the trachea.

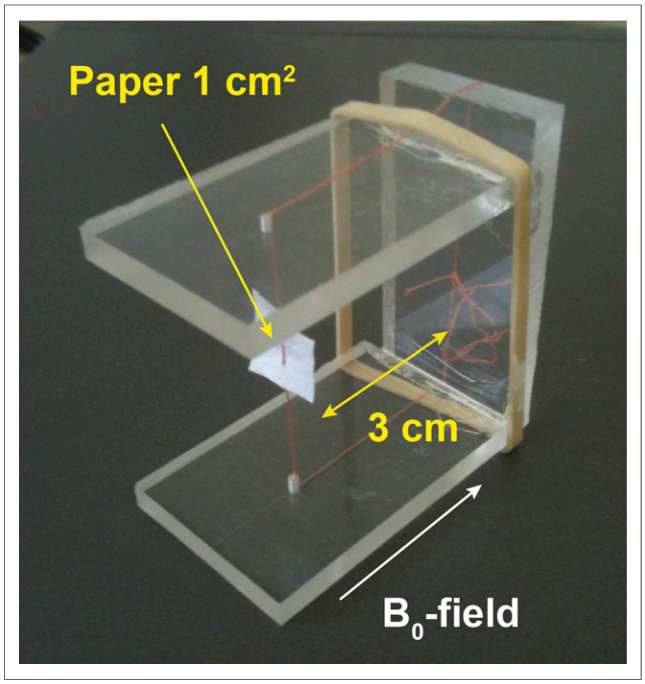

FIGURE 1. Acrylic glass device.

Sequential PET/CT measurements were started with a mean (±SD) residual activity of 272 ± 19 kBq/mL for each lesion with a PET acquisition time of 10 min. CT data were acquired with a low-dose protocol and reconstructed with an isotropic voxel size of 1.0 mm^3. Simultaneous PET/MR imaging measurements were performed afterward (10 min/acquisition); the residual activities for the lesions were 110 ± 9 kBq/mL. A 15-min MR imaging sequence followed: localizer,

TABLE 2
Volume-of-Interest Values for Various Lesions in Trachea and Larynx

Angle	Volume of interest	Volume (mm^3)	Mean (a.u.)	SD (a.u)	Distance L–A (cm)	A/L (%)	Ac/Lc (%)
20°	Trachea	464.8	2.36×10^{-2}	2.56×10^{-3}	—	—	—
	Upper artifact	500.0	4.90×10^{-3}	2.56×10^{-3}	2.0	20.8	19.3
	Lower artifact	388.7	4.95×10^{-3}	3.21×10^{-3}	2.0	21.0	25.1
	Epiglottis	849.6	8.83×10^{-3}	2.01×10^{-2}	—	—	—
	Artifact tubercle	714.8	3.43×10^{-3}	3.52×10^{-3}	3.0	38.9	46.2
35°	Trachea	527.3	1.49×10^{-2}	1.91×10^{-2}	—	—	—
	Upper artifact	414.1	4.29×10^{-3}	4.13×10^{-3}	1.5	28.8	36.7
	Lower artifact	304.7	4.54×10^{-3}	2.88×10^{-3}	1.5	30.4	52.7
	Epiglottis	541.0	1.01×10^{-2}	1.97×10^{-2}	—	—	—
	Artifact tubercle	369.1	4.62×10^{-3}	4.38×10^{-3}	2.5	46.6	67.0

a.u. = arbitrary units; L = lesion volume of interest; A = artifact volume of interest; A/L = ratio between activities within artifact volume of interest and lesion volume of interest; Ac/Lc = ratio between activity concentrations within artifact volume of interest and lesion volume of interest.

FIGURE 2. PET/MR-measured larynx at 20°.

T1-weighted 3-dimensional fast low-angle shot, ultrashort echo, and T1-weighted magnetization-prepared rapid gradient echo. The trachea with larynx was measured at 20° and 35° with respect to the magnetic field. Definition of volumes of interest for each lesion was based on the reconstructed MR images and the PET image with the artifacts. The shine-through effect was quantified as the ratio between the activities within the artifact volume of interest and the true lesion volume of interest (*13*). The ratio between the activity concentrations in both volumes of interest was also computed.

RESULTS

Phantom Measurements

Table 1 shows the activity ratio between the reconstructed activities in the paper and the backplane. The higher the maximum positron energy, the larger the number of annihilations on the backplane. Even for ^{18}F, a large percentage (47.6%) of the total activity was measured in the backplane. For ^{68}Ga, the apparent activity distribution was 5.7 times higher than the true one.

Measurements of Swine Organs

In the PET/MR images of the lungs (not shown) no shine-through was observed, only a change in the shape of the activity distribution: instead of the spheric shape visible on PET/CT, PET/MR showed the reconstructed lesions as significantly stretched along the magnetic field, whereas the size was contracted in the perpendicular direction.

Data on the trachea with larynx are listed in Table 2, and the corresponding images are shown in Figures 2 and 3. The lesion in the epiglottis is visible in Figure 2, as well as a shine-through artifact at the opposite side of the airway along the magnetic field. The artifact-to-lesion volume-of-interest ratio was 38.8% and 46.6% for the 2 orientations, respectively, which translated into activity concentration ratios of 46.2% and 67.0%. On the other hand, no shine-through was observed in the corresponding PET/CT images. For the trachea (Fig. 3), 2 artifacts were visible in the PET/MR images at the airway boundaries along the magnetic field. The artifact-to-lesion volume-of-interest ratio percentage, averaged over the 2 shine-through lesions, was 20.9% and 29.6% for 20° and 35°, respectively. In all cases, the apparent activity of the shine-through was smaller than the activity in the true lesion.

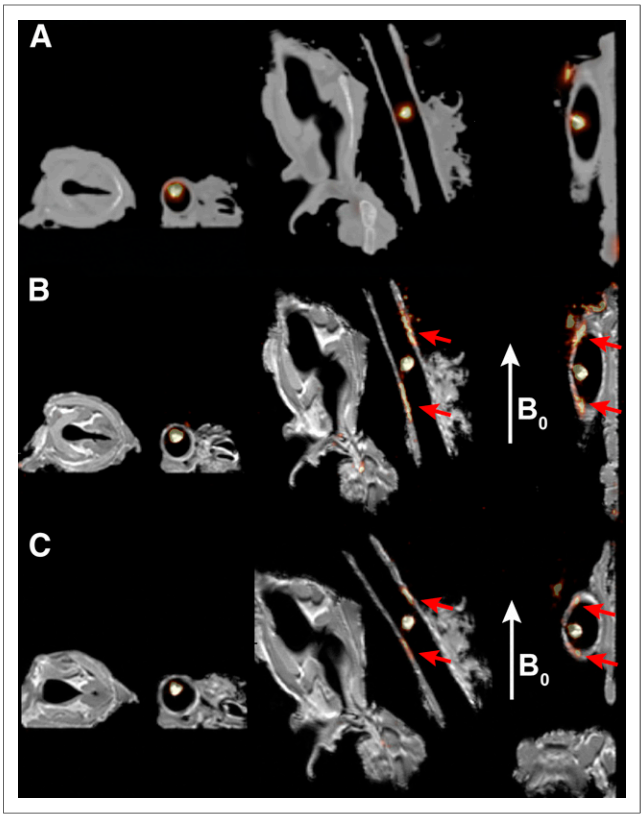

FIGURE 3. Measured trachea: PET/CT (A) and PET/MR images at 20° (B) and 35° (C). Red arrows show artifacts.

DISCUSSION

No shine-through was observed in the lungs because of their nonnegligible positron attenuation coefficient. Under the high magnetic field environment of PET/MR, shine-through artifacts were visible when the activity was placed very close to or inside an air cavity. Since these artifacts are a consequence of the helical path of positrons along the magnetic field, the shine-through was identifiable only in sagittal or coronal slices. As expected, the magnitude of the shine-through depended on the radioisotope (i.e., its positron maximum energy), as well as on the distance between the true source and the next tissue boundary: the shorter the path, the more intense the shine-through. Contrary to Abdul-Fatah et al. (*13*), no artifacts were observed in the PET/CT images, probably due to the shorter positron range of ^{68}Ga than of ^{124}I.

CONCLUSION

In clinical PET/MR, shine-through effects may become relevant when radiopharmaceuticals based on high-energy positron emitters are used and accumulate close to air cavities. In addition to false lesions, the positron shine-through also implies an apparently reduced uptake in the true location. The possible use of ^{124}I for antibody labeling or thyroid imaging, and the increasing interest in ^{68}Ga-labeled somatostatin analogs for PET/MR, makes it necessary to become aware of this potential problem. ^{68}Ga-DOTA peptides are commonly used for patients with meningiomas, which may infiltrate into the paranasal and nasal cavities (*19*). Given that ^{68}Ga-DOTATOC is also being used for PET/MR-based intensity-modulated radiation therapy planning for meningioma (*20*),

unidentified shine-through artifacts could also lead to irradiation of healthy brain tissue with critical function. Recognition of these artifacts is thus decisive. Additionally, for correct lesion detection, uptake quantification, or dosimetry, there is a need to apply positron-range correction methods able to take into account the density and boundaries of tissues and the effects of the magnetic field.

DISCLOSURE

The costs of publication of this article were defrayed in part by the payment of page charges. Therefore, and solely to indicate this fact, this article is hereby marked "advertisement" in accordance with 18 USC section 1734. This work was financially supported by the German Research Association (DFG) (grant PI771/3-1). No other potential conflict of interest relevant to this article was reported.

REFERENCES

1. Disselhorst JA, Bezrukov I, Kolb A, Parl C, Pichler BJ. Principles of PET/MR imaging. *J Nucl Med.* 2014;55(suppl 2):2S–10S.
2. Delso G, Fürst S, Jakoby B, et al. Performance measurements of the Siemens mMR integrated whole-body PET/MR scanner. *J Nucl Med.* 2011;52:1914–1922.
3. Levin C, Glover G, Deller T, McDaniel D, Peterson W, Maramraju SH. Prototype time-of-flight PET ring integrated with a 3T MRI system for simultaneous whole-body PET/MR imaging [abstract]. *J Nucl Med.* 2013;54(suppl 2):45P.
4. Iida H, Kanno I, Miura S, Murakami M, Takahashi K, Uemura K. A simulation study of a method to reduce positron annihilation spread distributions using a strong magnetic field in positron emission tomography. *IEEE Trans Nucl Sci.* 1986;33:597–600.
5. Hammer BE, Christensen NL, Heil BG. Use of a magnetic field to increase the spatial resolution of positron emission tomography. *Med Phys.* 1994;21:1917–1920.
6. Raylman R, Hammer B, Christensen NL. Combined MRI-PET scanner: a Monte Carlo evaluation of the improvements in PET resolution due to the effects of a static homogeneous magnetic field. *IEEE Trans Nucl Sci.* 1996;43:2406–2412.
7. Wirrwar A, Vosberg H, Herzog H, Halling H, Weber S, Muller-Gartner H-W. 4.5 tesla magnetic field reduces range of high-energy positrons: potential implications for positron emission tomography. *IEEE Trans Nucl Sci.* 1997;44: 184–189.
8. Peng H, Levin CS. Study of PET intrinsic spatial resolution and contrast recovery improvement for PET/MRI systems. *Phys Med Biol.* 2012;57:N101–N115.
9. Shah NJ, Herzog H, Weirich C, et al. Effects of magnetic fields of up to 9.4 T on resolution and contrast of PET images as measured with an MR-BrainPET. *PLoS ONE.* 2014;9:e95250.
10. Burdette D, Chesi E, Clinthorne NH, et al. Very high resolution small animal PET in strong magnetic fields. In: *2006 IEEE Nuclear Science Symposium Conference Record*. Piscataway, NJ: IEEE; 2006:2417–2420.
11. Soultanidis G, Karakatsanis N, Nikiforidis G, Loudos G. Study of the effect of magnetic field in positron range using GATE simulation toolkit. *J Phys Conf Ser.* 2011;317:012021.
12. Watson CC, Eriksson L, Kolb A. Physics and applications of positron beams in an integrated PET/MR. *Phys Med Biol.* 2013;58:L1–L12.
13. Abdul-Fatah SB, Zamburlini M, Halders SGEA, Brans B, Teule GJJ, Kemerink GJ. Identification of a shine-through artifact in the trachea with ^{124}I PET/CT. *J Nucl Med.* 2009;50:909–911.
14. Burdette D, Albani D, Chesi E, et al. PET artifacts from off-plane sources in high magnetic fields. In: *2008 IEEE Nuclear Science Symposium Conference Record*. Piscataway, NJ: IEEE; 2008:3769–3774.
15. Kraus R, Delso G, Ziegler SI. Simulation study of tissue-specific positron range correction for the new Biograph mMR whole-body PET/MR system. *IEEE Trans Nucl Sci.* 2012;59:1900–1909.
16. Kolb A, Wehrl HF, Hofmann M, et al. Technical performance evaluation of a human brain PET/MRI system. *Eur Radiol.* 2012;22:1776–1788.
17. Hong IK, Chung ST, Kim HK, Kim YB, Son YD, Cho ZH. Ultra fast symmetry and SIMD-based projection-backprojection (SSP) algorithm for 3-D PET image reconstruction. *IEEE Trans Med Imaging.* 2007;26:789–803.
18. Schwaiger M, Ziegler S, Nekolla SG. PET/CT: challenge for nuclear cardiology. *J Nucl Med.* 2005;46:1664–1678.
19. Ho KL. Primary meningioma of the nasal cavity and paranasal sinuses. *Cancer.* 1980;46:1442–1447.
20. Thorwarth D, Henke G, Müller A-C, et al. Simultaneous ^{68}Ga-DOTATOC-PET/MRI for IMRT treatment planning for meningioma: first experience. *Int J Radiat Oncol Biol Phys.* 2011;81:277–283.